Detection of Heavy Metal Ions in Drinking Water Using a High-Resolution Differential Surface Plasmon Resonance Sensor

ERICA S. FORZANI,[†] HAIQIAN ZHANG,[†] WILFRED CHEN,[‡] AND NONGJIAN TAO*,[†]

Department of Electrical Engineering & The Center for Solid State Electronics Research, Arizona State University, Tempe, Arizona 85287, and Department of Chemical and Environmental Engineering, University of California, Riverside, California 92521

We have built a high-resolution differential surface plasmon resonance (SPR) sensor for heavy metal ion detection. The sensor surface is divided into a reference and sensing areas, and the difference in the SPR angles from the two areas is detected with a quadrant cell photodetector as a differential signal. In the presence of metal ions, the differential signal changes due to specific binding of the metal ions onto the sensing area coated with properly selected peptides, which provides an accurate real-time measurement and quantification of the metal ions. Selective detection of Cu^{2+} and Ni^{2+} in the ppt−ppb range was achieved by coating the sensing surface with peptides NH_2-Gly-Gly-His-COOH and NH_2-$(His)_6$-COOH. Cu^{2+} in drinking water was tested using this sensor.

Introduction

The detection and quantification of heavy metal ions are important in many applications, including environmental monitoring, waste management, developmental biology, and clinical toxicology. A number of techniques have been developed over the years for heavy metal ion analysis, including atomic absorption spectrometry [1], inductively coupled plasma mass spectrometry [2], anodic stripping voltammetry [1, 3, 4], X-ray fluorescence spectrometry [5], and microprobes [6]. These techniques in general require expensive equipment, sample pretreatment, and/or analyte preconcentration steps. Therefore, a simple, rapid, inexpensive, selective, and sensitive method that permits real-time detection of metal ions is still a challenging goal. In addition, due to the danger that the heavy metal ions pose to operators, minimal sample handling is desirable.

To design highly selective metal ion sensors, several innovative recognizing elements based on organic chelators [7], organic polymers [8], proteins [9], peptides [3, 10−13], cells [14], and DNA/RNA [15] have been developed. Peptides are particularly attractive for this purpose since combinatorial chemistry can be used to find optimal amino acid sequences for specific metal-ion recognition. A highly specific molecular recognition element must be matched with a sensitive detector to convert the specific metal-ion recognition event into an electrical, mechanical, or optical signal. Surface plasmon resonance (SPR) is one of the most sensitive methods for detection of analyte binding events [16, 17]. SPR is based on detecting the resonance of surface plasmons, or collective oscillations of electrons, in a metallic film with light. Because the resonance condition is extremely sensitive to the refractive index of the medium adjacent to the metallic film, the presence of analyte molecules on the surface of the metallic film can be accurately detected [18, 19]. High specificity of SPR sensors is usually achieved by modifying the metal surface with a layer of appropriate ligand molecules as recognizing elements, such as those mentioned above [20−22]. Once molecules bind to the surface, SPR sensors can also be used to study conformational changes of surface-bound molecules [23].

We have recently reported on a simple SPR sensor that achieves high resolution by using a bicell or a quadrant cell photodetector [18, 19, 24]. These setups allowed us to achieve an angular resolution of 10^{-5} deg. Particularly, the use of quadrant cell detection allowed us to reduce mechanical vibrations, thermal drifts, and the influence of the refractive index changes in the bulk solution [18]. In this paper, we demonstrate the selective detection of different metal ions in the ppb and ppt ranges by combining the high-resolution SPR with highly selective peptides as molecular recognition elements.

Experimental Section

Instrumentation. We have described the SPR setup in detail in ref *18.* Briefly, the setup is based on Kretschmann configuration, in which a p-polarized laser beam ($\lambda = 635$ nm) is focused through a prism onto a metal film placed on the prism. Because the incident beam is focused, it spans over a range of incident angles depending on the focal distance and beam width. At the so-called resonance angle, the incident light is absorbed by the surface plasmon, and the reflection drops to a minimum, which results in a thin dark line known as the SPR dip (Figure 1A). We use a gold film that is divided into a sensing area and a reference area. The SPR dips from the two areas are simultaneously monitored by a quadrant cell photodetector, containing four nearly identical photocells (A, B, C, and D). The resonance angles from the sensing and reference areas are detected by differential signals, $(A - B)/(A + B)$ and $(C - D)/(C + D)$, respectively, which are recorded with a digital oscilloscope (Yokogawa, DL708). Prior to each measurement, the prism is rotated to bring the SPR dip to the center of the reflected beam, and the quadrant photodetector is adjusted to balance not only A and B for the sensing signal but also C and D for the reference signal (Figure 1B). When the analyte is injected into the cell, both the sensing and the reference SPR dips shift due to the small but finite change in the solution refractive index. However, since the sensing area is modified with metal ion recognizing molecules, specific binding of metal ions onto the sensing area causes an additional dip shift. The differential signal, $(A - B)/(A + B) - (C - D)/(C + D)$ eliminates the effect due to the solution refractive index change, which allows us to detect the specific metal ion binding with an accuracy of 10^{-5} deg (Figure 1B). Because the four photocells (on a single chip) are nearly identical, thermal drift and mechanical noises are also subtracted out, thus providing a simple, rapid, and accurate method to detect metal ions [18].

Gold Film Modification. The gold film (∼50 nm thick) was evaporated on BK7 glass slides by an ion beam coater (model 681, Gatan Inc.). The film was separated in two parts

* Corresponding author phone: (480)965-4456; fax: (480)965-8118; e-mail: nongjian.tao@asu.edu.
† Arizona State University.
‡ University of California, Riverside.
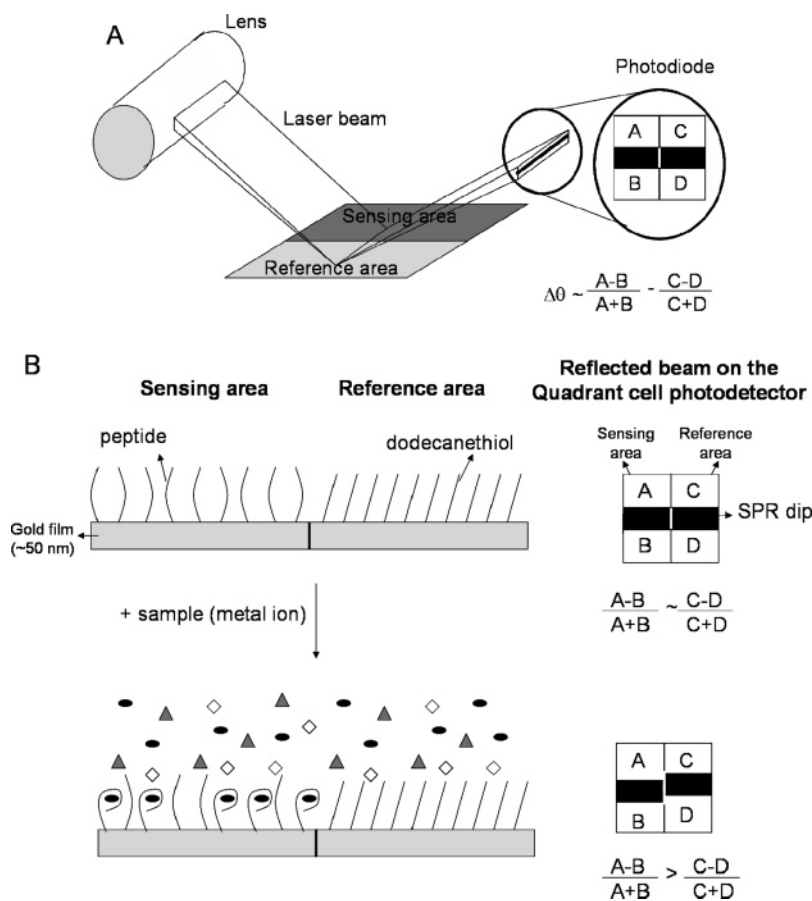
FIGURE 1. Schematic representation of the differential SPR setup. (A) A diode laser is focused with a cylindrical lens through a prism onto the gold film supported on the prism (not shown for clarity). The gold film is divided into a sensing area and a reference area. The reflected beams from the two areas have dark lines (SPR dips), corresponding to resonance of surface plasmon, when the incident angle is appropriately adjusted. A quadrant cell photodetector simultaneously measures the SPR dips from the reference (C, D) and sensing (A, B) areas. (B) Prior to each measurement, the quadrant photodetector is adjusted to balance A, B, C, and D, so that $(A - B)/(A + B) - (C - D)/(C + D) \sim 0$. When the analyte is injected into the cell, the specific adsorption of metal ions onto the sensing area causes a shift in the SPR dip position, which is detected by the differential signal $(A - B)/(A + B) - (C - D)/(C + D)$.
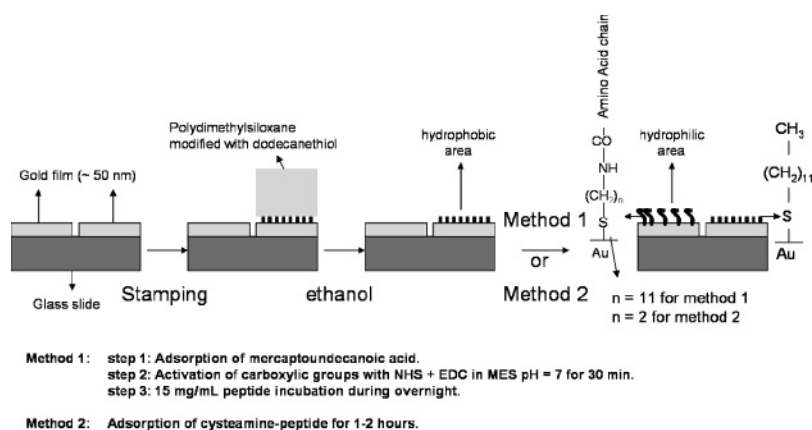
FIGURE 2. Schematic representation of the different routes to modify the sensing and reference areas. The sensing area was modified with short peptides using two methods, while the reference area was modified with dodecanethiol self-assembled monolayer using PDMS stamping (see Experimental Section for details).

with a gap of $100-200\,\mu$m. One part was modified as reference area with a self-assembled monolayer of 1-dodecanethiol (DDT) (Aldrich) using a poly(dimethylsiloxane) (PDMS) stamp, and the second part was designated as sensing area. After modification with DDT, the reference part became hydrophobic, which prevented the adsorption of hydrophilic species. The sensing area was modified with short peptides chosen to sense specifically copper and nickel ions. Two different kinds of modification procedures were used to

immobilize the peptides on the sensing area. The first one (method 1) was carried out similarly to ref 3 while the second one (method 2) comprised the chemisorption of synthesized cysteamine-modified peptides (Figure 2). Method 1 included the following steps: (a) overnight incubation of the gold film in 1mM 11-mercaptoundecanoic acid (MUA) (Sigma) ethanolic solution followed by rinsing with ethanol; (b) activation of the carboxylic groups by incubation of the MUA-modified gold surface in 0.1 M 2-(morpholino)ethanesulfonic acid

(MES) (Sigma) buffer solution (pH 7) containing 15 mM N-hydroxysuccinimide (NHS) (Sigma) and 75 mM 1-ethyl-3-(3-dimethylaminopropyl)carbodiimide hydrochloride (EDC) (Sigma) for 30 min; and (c) peptide immobilization on a NHS-activated surface by incubation in a 15 mg/mL NH$_2$-Gly-Gly-His-COOH (Bachem) solution prepared in MES pH 7 or a 15 mg/mL synthesized NH$_2$-(His)$_6$-COOH solution prepared in DMF. The immobilization following method 2 was carried out by placing 200−300 μL of 46 mM peptide aqueous solution on the sensing area for 1−2 h while the reference area was masked with DDT-modified PDMS stamp.

The peptides NH$_2$-(His)$_6$-COOH (for method 1), NH$_2$-Gly-Gly-His-cysteamine (for method 2) and NH$_2$-(His)$_6$-cysteamine (for method 2) were synthesized on a Milligen 9050 using a peptide continuous-flow and F_{moc} chemistry with HCTU [2-(1H-6-chlorobenzotriazol-1-yl)-1,1,3,3-tetramethyluronium hexafluorophosphate] as coupling reagent. In the case of cysteamine peptides, a cysteamine 4-methoxytrityl resin (Novabiochem, La Jolla, CA) was used. Synthesis reagents were purchased from Applied Biosystems (Foster City, CA), AnaSpec (San Jose, CA), and Peptides International (Louisville, KY). The synthetic peptides were cleaved from the resin with 95% triflouroacetic acid containing 2.5% triisopropylsilane and 2.5% water. After that, the cleavage solvent was evaporated in a SpeedVac vacuum centrifuge (Savant Instruments, Holbrook, NY). The sample was then diluted with diethyl ether, causing part of the peptide to precipitate. A second peptide fraction was extracted from the ether solution with water, followed by drying the aqueous solution in the SpeedVac. Mass spectra were performed to check final molecular weight of the synthesized peptides (see Supporting Information). NH$_2$-Gly-Gly-His-cysteamine was purified through HPLC. Cysteamine peptide concentrations were assessed spectrophotometrically by determining thiol group concentration through oxidation with 5,5′-dithiobis-(2-nitrobenzene) (Ellman's reagent).

Copper and Nickel Ion Detections. Gly-Gly-His-modified sensing areas (11) were used to detect Cu^{2+} while (His)$_6$-modified films (25) were employed to sense Ni^{2+}. To evaluate the degree of specificity for each metal ion, cross interference studies were performed. The response of the SPR sensors were tested in deionized water (Nanopure, 18 MΩ·cm) upon successive injections of different concentrations (800 pM−100 μM) of metal ion solutions (Cu(NO$_3$)$_2$ (Aldrich) and NiCl$_2$ (Aldrich)) prepared in deionized water. All the solutions were prepared in ultracentrifuge plastic tubes previously treated with 6 M nitric acid and thoroughly washed with ultrapure water using calibrated micropipets. The sample cell in which the gold film was mounted was made of Teflon. A 10 μL sample solution was injected into the sample cell, and the SPR response was monitored and recorded continuously during the process.

Results and Discussion

Nickel and Copper Ion Detection. Figure 3 shows the time course of the differential signal (A − B)/(A + B) − (C − D)/(C + D) upon introduction of nickel ions into the sample cell. The sensing area was modified with (His)$_6$-cysteamine according to method 2. The increase in the differential signal after each Ni^{2+} injection indicates that the specific binding of Ni^{2+} on (His)$_6$ takes place. The measurement is sensitive enough to detect the specific binding of Ni^{2+} in real time from solution concentrations as low as 41 pM (2.4 ppt) without preconcentration or stirring the solution.

Figure 4 (curve for method 2) shows the corresponding differential signal change as a function of Ni^{2+} concentration. A linear response with a sensitivity of (0.0020 ± 0.0001) deg/nM, and a regression coefficient of 0.9854 is observed. The results obtained onto a MUA-(His)$_6$-modified gold surface
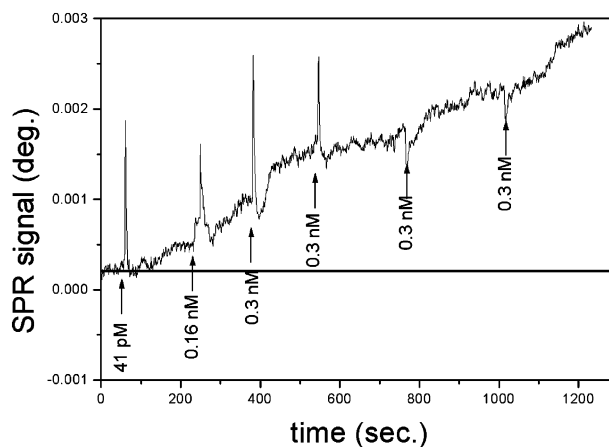
FIGURE 3. Time course of the SPR differential signal (A − B)/(A + B) − (C − D)/(C + D) upon Ni^{2+} injections. The sensing area is modified with a monolayer of (His)$_6$-cysteamine, and the reference area is covered with a self-assembled monolayer of DDT. The Ni^{2+} concentrations added to the solution cell in each injection are indicated.
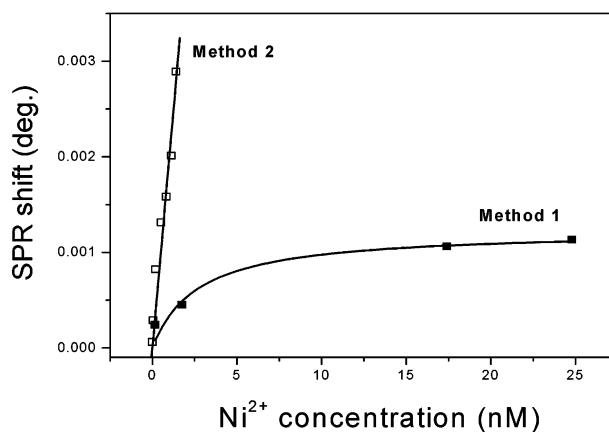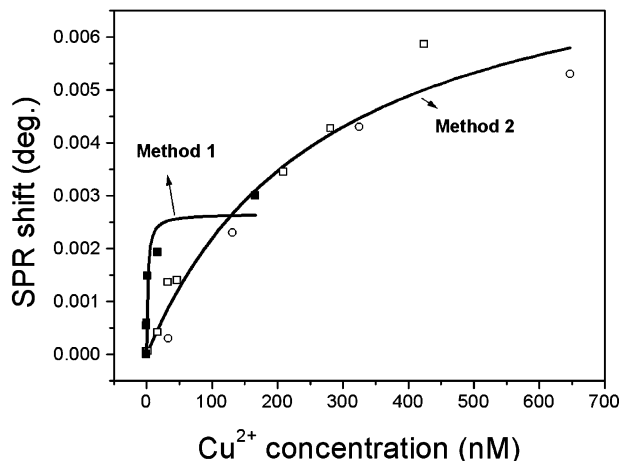

FIGURE 4. SPR differential signal change as a function of Ni^{2+} concentration onto a MUA-(His)$_6$ (method 1, ■) and cysteamine-(His)$_6$ (method 2, □) modified sensing area. Full lines show the corresponding fitting to eq 1.

(method 1) under similar conditions are also shown for comparison. In this case, the sensitivity is lower than that obtained on films resulting from method 2, which indicates that method 2 is more effective than method 1 to produce good surface coverage of (His)$_6$. However, the detection limit achieved by method 1 is still low (178 pM or 10.4 ppt). The Langmuir-like features defined in the response for method 1 are summarized in Table 1 (see details below).

In parallel, the analytical response toward Cu^{2+} on Gly-Gly-His-modified gold surfaces was studied. The time course of the differential signal (A − B)/(A + B) − (C − D)/(C + D) showed similar features to those shown in Figure 3 (not shown) that demonstrate the ability of our SPR sensor to detect trace amount of Cu^{2+} in real time. Figure 5 shows the typical response of Gly-Gly-His-modified SPR sensors as a function of Cu^{2+} concentration by using both immobilization methods (method 1 and 2). Method 2 gives a wider dynamic range (limited by saturation of Cu^{2+} binding), but its detection limit (0.1 ppb) is not as good as that achieved by method 1 (∼2 ppt). The analytical parameters assessed for Gly-Gly-His-cysteamine (method 1) could not be improved even after further peptide purification (HPLC). Thus, thermodynamic affinity constants (K) for copper binding on the peptide

TABLE 1. Comparative Analytical Performance and Thermodynamic Parameters for Different Surface Modifications

| immobilization method	(His)$_6$-Ni^{2+}		Gly-Gly-His-Cu^{2+}	
	detection limit	thermodynamic parameters	detection limit	thermodynamic parameters
1 (MUA-NHS activation)	178 pM (10.4 ppt)	$\Delta\theta_{sat} = (0.0012 \pm 0.0001)$ deg $K = (4 \pm 2) \times 10^8$ M^{-1}	32 pM (2.0 ppt)	$\Delta\theta_{sat} = (0.0027 \pm 0.0003)°$ $K = (6 \pm 1) \times 10^8$ M^{-1}
2 (chemisorption through thiol bond)	41 pM (2.4 ppt)	sensitivity = (0.0020 ± 0.0001) deg/nM	1.6 nM (0.10 ppb)	$\Delta\theta_{sat} = (0.008 \pm 0.001)°$ $K = (4 \pm 1) \times 10^6$ M^{-1}

FIGURE 5. SPR differential signal change as a function of Cu^{2+} concentration onto a MUA-Gly-Gly-His (method 1) and cysteamine-His-Gly-Gly (method 2) modified sensing area. Full lines show the corresponding fitting to eq 1. Symbols □ and ○ for method 2 represent data taken from independent experiments performed with different SPR sensors built up under the same conditions.

modified surfaces resulting from both immobilization methods were estimated by using Langmuir-like equation:

$$\Delta\theta = \Delta\theta_{sat}C(M^{2+})/((1/K) + C(M^{2+})) \qquad (1)$$

where $\Delta\theta$ is the SPR shift, $\Delta\theta_{sat}$ is the SPR shift at the saturation, and $C(M^{2+})$ is the metal ion concentration, respectively (Table 1). This equation assumes that the SPR shift is proportional to the number of bound metal ions, the binding sites are independent, and the complexation equilibrium is given by:

$$\text{Au-peptide} + M^{2+}(aq) \rightleftarrows \text{Au-(peptide-}M^{2+}) \qquad (2)$$
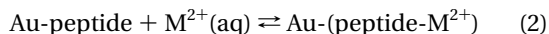
The value of K found for copper binding on Au/MUA/Gly-Gly-His ($\sim 6 \times 10^8$ M^{-1}) was higher than that for copper on Au/cysteamine/His-Gly-Gly ($\sim 4 \times 10^6$ M^{-1}) [The affinity constant values (K) estimated under these conditions could be "apparent" K since the SPR signal change obtained for each binding metal concentration could be still under kinetic control rather than being at equilibrium.], which indicates a more effective Cu^{2+} binding for MUA-Gly-Gly-His (method 1). Figure 6 shows the chemical structure of both ligands (MUA-Gly-Gly-His and cysteamine-His-Gly-Gly) after immobilization procedure. Although the immobilized peptide (NH$_2$-Gly-Gly-His-COOH) is the same in both cases, a steric impediment could cause a weaker Cu^{2+} binding in the case of cysteamine-His-Gly-Gly-NH$_2$ (B), since His is closer to gold surface. However, the lower affinity constant in this case gives a higher dynamic range required for copper detection in real samples.

Table 1 summarizes the analytical performance of the (His)$_6$ and Gly-Gly-His SPR sensors for Ni^{2+} and Cu^{2+} detections using different peptide immobilization methods. The best sensitivity achieved for Ni^{2+} detection was the Au
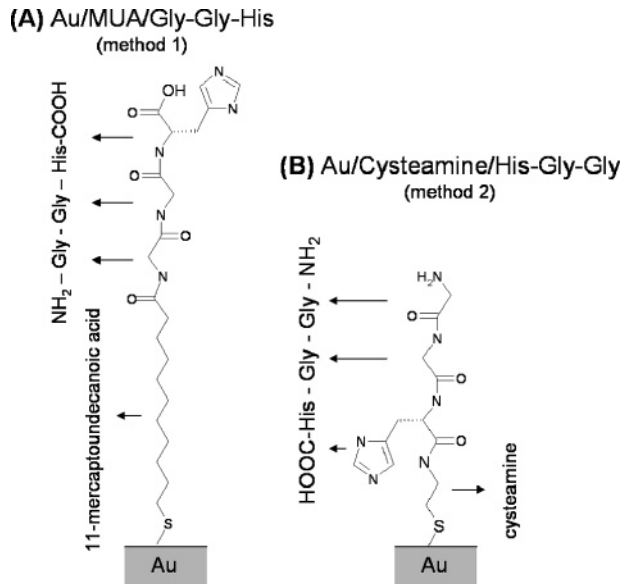
FIGURE 6. Schematic representation of the chemical structure of NH$_2$-Gly-Gly-His-COOH after immobilization procedure through (A) method 1 (MUA-NHS activation) and (B) method 2 (chemisorption through thiol bond).

film modified with (His)$_6$ through thiol-Au bond. In this case the SPR signal was out of scale before the surface was saturated, which prevented us from estimating the Ni^{2+} binding affinity constant. The rest of the sensors showed Langmuir-type adsorption isotherm which means that a calibration plot of the response reciprocal versus concentration reciprocal would be the better way to use for sample analysis. However, the matrix of real samples can change the specific adsorption features, so that this table gives us only a rough idea about the analytical performance of the SPR sensors (see Copper Analysis in Drinking Water). To check the reproducibility of the SPR sensors, we have performed the measurements using different gold films. Figure 5 shows an example of two separate measurements (□ and ○ in Figure 5) that are in good agreement with each other.

Interference Analysis and Stability. To use peptide-modified SPR sensors for routine analysis, a number of factors must be addressed in addition to sensibility, detection limits and reproducibility described above. These include the interference from metal ions in real samples and reusability of the sensing surface.

Cu^{2+} can be a serious interference for Ni^{2+} detection (and vice versa) since both ions form square planar 4N complexes with peptides in solution (25). Therefore, we decided to study the Ni^{2+}−Cu^{2+} cross interference. We tested the response of Cu^{2+} and Ni^{2+} on MUA-(His)$_6$- and MUA-Gly-Gly-His-modified surfaces, respectively. Exposure of (His)$_6$-modified surface to Cu^{2+} did not produce SPR response (<170 nM), showing that (His)$_6$ is selective for Ni^{2+} detection. However, Gly-Gly-His surface is sensitive to both Cu^{2+} and Ni^{2+}. For example, 170 nM Ni^{2+} on Gly-Gly-His produced a SPR response that is about half of the response obtained for Cu^{2+}
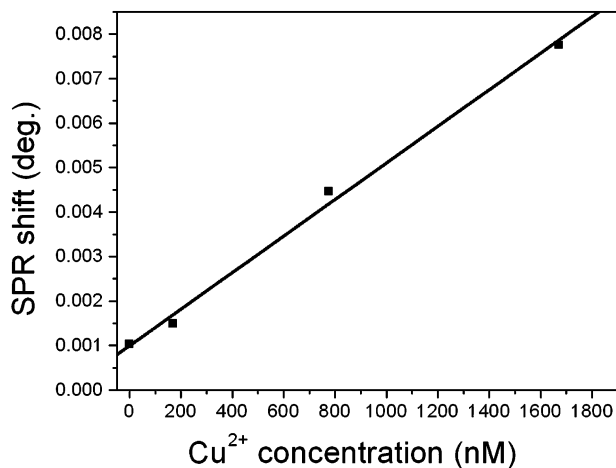
FIGURE 7. Calibration plot for Cu^{2+} internal standard addition analysis of drinking water using a SPR sensor built with cysteamine-His-Gly-Gly (method 2) modified sensing area.

with the same concentration on the same peptide. Since, $(His)_6$ films were selective for Ni^{2+}, an array of sensors containing both $(His)_6$ and Gly-Gly-His may solve the Ni^{2+} interference problem on Gly-Gly-His. We did not investigate the contribution of other potential interference species. However, previous published works have demonstrated that there is no binding between the Gly-Gly-His and other ions such as Co^{2+}, Pb^{2+}, Ba^{2+}, Cd^{2+}, Ca^{2+}, Fe^{3+}, Zn^{2+}, and Hg^{2+} (11).

As for the reusability of the sensing surface (Au film), we observed that it is possible to regenerate the peptide-modified surface and to obtain a similar response (93%) by dipping the modified surface in 0.1 M perchloric acid for 30 s. Furthermore, the SPR sensor stored at room temperature can be reused at least 1 week later.

Copper Analysis in Drinking Water. We have tested the ability of our SPR sensor to analyze Cu^{2+} in drinking water (tap water) (Ni^{2+} in drinking water is negligible) (26). Control of Cu^{2+} levels in drinking water is important since short-term exposure of high Cu^{2+} levels produces gastrointestinal distress while long-term exposure generates liver or kidney damage. Cu^{2+} levels are critical for people with Wilson's disease since they need to know if the normal copper ion levels of drinking water exceed the action level. Normally, Cu^{2+} levels are checked in drinking water plants to ensure that copper concentration is lower than 1.3 ppm (maximum permitted by EPA) (26). However, erosion of water deposits and corrosion of plumbing systems can dramatically increase the local concentrations. So a simple, fast, and accurate sensor that can test both local tap water and distribution system water is necessary. To perform drinking water analysis, we found that Gly-Gly-His-cysteamine modified surfaces (method 2) have better dynamic range and that the sample needed a dilution factor of ~20 at least. Thus, the injection of 15 μL of tap water to 300 μL of deionized water was good to detect Cu^{2+} coming from drinking water. Figure 7 shows the internal standard addition analysis performed on one of the samples. The average Cu^{2+} concentration for two water samples taken from the same tap along 1 week was (0.34 ± 0.03) ppm, which is consistent with the finding by atomic absorption spectroscopy. This Cu^{2+} content is 6 times higher than that declared by the water plant (27), which could indicate additional Cu^{2+} from the distribution system.

We noted that the calibration plots for Cu^{2+} in drinking water were different from that obtained in deionized water (Figure 5). The calibration plots of the standard internal addition analysis were linear up to 2.1 μM Cu^{2+} ion concentrations and showed an important sample matrix

effect on the Cu^{2+} binding. The linear response simplifies the data analysis since a test consisting of one injection of sample and one injection of Cu^{2+} standard is accurate enough to determine drinking water Cu^{2+} content.

In summary, we have demonstrated a method to analyze metal ions in drinking water by combining a high-performance differential SPR with surface modification of short peptides. In comparison to other techniques, such as atomic absorption spectrometry, our SPR sensors are simple, low cost and portable, yet with high sensitivity without the need of sample preconcentration or pretreatment, so we believe that the SPR sensor may be a good alternative for testing metal ion in drinking water.

Supporting Information Available

Mass spectral characterization (MALDI TOF) of synthesized peptides used in SPR sensor (method 2). This material is available free of charge via the Internet at http://pubs.acs.org.

Literature Cited

(1) Bannon, D. I.; Chisolm, J. J. Anodic stripping voltammetry compared with graphite furnace atomic absorption spectrophotometry for blood lead analysis. *Clin. Chem.* **2001**, *47* (9), 1703−1704.

(2) Liu, H. W.; Jiang, S. J.; Liu, S. H. Determination of cadmium, mercury and lead in seawater by electrothermal vaporization isotope dilution inductively coupled plasma mass spectrometry. *Spectrochim. Acta, Part B* **1999**, *54* (9), 1367−1375.

(3) Yang, W. R.; Chow, E.; Willett, G. D.; Hibbert, D. B.; Gooding, J. J. Exploring the use of the tripeptide Gly-Gly-His as a selective recognition element for the fabrication of electrochemical copper sensors. *Analyst* **2003**, *128* (6), 712−718.

(4) Baldo, M. A.; Daniele, S.; Ciani, I.; Bragato, C.; Wang, J. Remote stripping analysis of lead and copper by a mercury-coated platinum microelectrode. *Electroanalysis* **2004**, *16* (5), 360−366.

(5) Eksperianova, L. P.; Blank, A. B.; Makarovskaya, Y. N. Analysis of waste water by X-ray fluorescence spectrometry. *X-ray Spectrom.* **2002**, *31* (3), 259−263.

(6) Arai, Y.; Lanzirotti, A.; Sutton, S.; Davis, J. A.; Sparks, D. L. Arsenic speciation and reactivity in poultry litter. *Environ. Sci. Technol.* **2003**, *37* (18), 4083−4090.

(7) Burdette, S. C.; Frederickson, C. J.; Bu, W. M.; Lippard, S. J. ZP4, an improved neuronal Zn^{2+} sensor of the Zinpyr family. *J. Am. Chem. Soc.* **2003**, *125* (7), 1778−1787.

(8) Wu, X. Q.; Kim, J.; Dordick, J. S. Enzymatically and combinatorially generated array-based polyphenol metal ion sensor. *Biotechnol. Prog.* **2000**, *16* (3), 513−516.

(9) Darwish, I. A.; Blake, D. A. Development and validation of a one-step immunoassay for determination of cadmium in human serum. *Anal. Chem.* **2002**, *74* (1), 52−58.

(10) Deo, S.; Godwin, H. A. A selective, ratiometric fluorescent sensor for Pb^{2+}. *J. Am. Chem. Soc.* **2000**, *122* (1), 174−175.

(11) Yang, W. R.; Jaramillo, D.; Gooding, J. J.; Hibbert, D. B.; Zhang, R.; Willett, G. D.; Fisher, K. J. Sub-ppt detection limits for copper ions with Gly-Gly-His modified electrodes. *Chem. Commun.* **2001**, *19*, 1982−1983.

(12) Shults, M. D.; Pearce, D. A.; Imperiali, B. Modular and tunable chemosensor scaffold for divalent zinc. *J. Am. Chem. Soc.* **2003**, *125* (35), 10591−10597.

(13) Mlynarz, P.; Valensin, D.; Kociolek, K.; Zabrocki, J.; Olejnik, J.; Kozlowski, H. Impact of the peptide sequence on the coordination abilities of albumin-like tripeptides towards Cu^{2+}, Ni^{2+} and Zn^{2+} ions. Potential albumin-like peptide chelators. *New J. Chem.* **2002**, *26* (2), 264−268.

(14) Shetty, R. S.; Ramanathan, S.; Li, Y.; Wolford, J.; Shah, P.; Daunert, S. Whole cell-based sensing systems for metal ions. *Abstr. Pap. Am. Chem. S.* **2001**, *221*, U92−U92.

(15) Lu, Y.; Liu, J. W.; Li, J.; Bruesehoff, P. J.; Pavot, C. M. B.; Brown, A. K. New highly sensitive and selective catalytic DNA biosensors for metal ions. *Biosens. Bioelectron.* **2003**, *18* (5−6), 529−540.

(16) Chinowsky, T. M.; Saban, S. B.; Yee, S. S. Experimental data from a trace metal sensor combining surface plasmon resonance with anodic stripping voltammetry. *Sens. Actuators B* **1996**, *35* (1−3), 37−43.

(17) Palumbo, A.; Pearson, C.; Nagel, J.; Petty, M. C. Surface plasmon resonance sensing of liquids using polyelectrolyte thin films. *Sens. Actuators B* **2003**, *91* (1−3), 291−297.

(18) Zhang, H. Q.; Boussaad, S.; Tao, N. J. High-performance differential surface plasmon resonance sensor using quadrant cell photodetector. *Rev. Sci. Instrum.* **2003**, *74* (1), 150−153.

(19) Wang, S.; Boussaad, S.; Tao, N. J. High sensitivity stark spectroscopy obtained by surface plasmon resonance measurement. *Anal. Chem.* **2000**, *72* (17), 4003−4008.

(20) Song, F. Y.; Zhou, F. M.; Wang, J.; Tao, N. J.; Lin, J. Q.; Vellanoweth, R. L.; Morquecho, Y.; Wheeler-Laidman, J. Detection of oligonucleotide hybridization at femtomolar level and sequence-specific gene analysis of the *Arabidopsis thaliana* leaf extract with an ultrasensitive surface plasmon resonance spectrometer. *Nucleic Acids Res.* **2002**, *30* (14).

(21) Sakai, T.; Shinahara, K.; Torimaru, A.; Tanaka, H.; Shoyama, Y.; Matsumoto, K. Sensitive detection of glycyrrhizin and evaluation

(22) Kobori, A.; Horie, S.; Suda, H.; Saito, I.; Nakatani, K. The SPR sensor detecting cytosine-cytosine mismatches. *J. Am. Chem. Soc.* **2004**, *126* (2), 557−562.

(23) Avilov, S. V.; Aleksandrova, N. A.; Demchenko, A. P. Quaternary structure of alpha-crystallin is necessary for the binding of unfolded proteins: A surface plasmon resonance study. *Protein Peptide Lett.* **2004**, *11* (1), 41−48.

(24) Tao, N. J.; Boussaad, S.; Huang, W. L.; Arechabaleta, R. A.; D'Agnese, J. High-resolution surface plasmon resonance spectroscopy. *Rev. Sci. Instrum.* **1999**, *70* (12), 4656−4660.

(25) Sigel, H.; Martin, R. B. Coordinating properties of the amide bond—stability and structure of metal-ion complexes of peptides and related ligands. *Chem. Rev.* **1982**, *82*, 2 (4), 385−426.

(26) www.epa.gov/safewater/mcl.html#mcls.

(27) www.tempe.gov/water/wqsum.htm.

of the affinity constants by a surface plasmon resonance-based immunosensor. *Anal. Sci.* **2004**, *20* (2), 279−283.